

LA-UR -82-1820

CONF-830103--4

Los Alamos National Laboratory is operated by the University of California for the United States Department of Energy under contract W-7405-ENG-36.

LA-UR--82-1820

DE82 018387

TITLE: THERMAL-HYDRAULIC ANALYSIS OF MAIN-STEAM-LINE-BREAK ACCIDENTS
AS POTENTIAL INITIATORS FOR REACTOR VESSEL

AUTHOR(S): David E. Lankin

DISCLAIMER

This report was prepared as an account of work sponsored by an agency of the United States Government. Therefore, the United States Government is authorized to reproduce and distribute reprints for government purposes, not withstanding any copyright notation that may appear hereon. It is understood that this report is to be distributed outside the government only by special arrangement with the publisher. The views and opinions of authors expressed herein do not necessarily state or reflect those of the United States Government or any agency thereof.

SUBMITTED TO: Second International Topical Meeting on Nuclear Thermal-Hydraulics, January 11-14, 1983, Santa Barbara, California

MASTER

DISTRIBUTION OF THIS DOCUMENT IS UNLIMITED

By acceptance of this article, the publisher recognizes that the U.S. Government retains a nonexclusive, royalty-free license to publish or reproduce the published form of this contribution, or to allow others to do so, for U.S. Government purposes.

The Los Alamos National Laboratory requests that the publisher identify this article as work performed under the auspices of the U.S. Department of Energy

Los Alamos Los Alamos National Laboratory
Los Alamos, New Mexico 87545

THERMAL-HYDRAULIC ANALYSIS OF MAIN-STEAM-LINE-BREAK
ACCIDENTS AS POTENTIAL INITIATORS FOR REACTOR VESSEL
PRESSURIZED THERMAL SHOCK*

by

D. Lamkin**

ABSTRACT

Results are presented from two thermal-hydraulic analyses of postulated main-steam-line breaks for the OCONEE nuclear power plant. One calculation assumes runaway feedwater supply, whereas normal feedwater management is used in the other. The analyses were performed with the TRAC-PD2 code. The objective was to provide primary coolant temperature and pressure histories to assist in evaluating possible reactor-vessel pressurized-thermal-shock concerns.

I. INTRODUCTION

Results are presented from two TRAC-PD2¹ calculations performed to predict the response of a Babcock-and-Wilcox (E&W) lowered-loop pressurized water reactor to a postulated main-steam-line-break (MSLB) accident. The particular

*Work performed under the auspices of the US Nuclear Regulatory Commission.

**Energy Division, Los Alamos National Laboratory, Los Alamos, NM 87545
Member ASME, ANS

plant modeled was basically TMI-2, but several key parameters were changed to approximate the Oconee¹ plant.

These calculations were motivated by NRC licensing concerns related to the "pressurized thermal shock" issue. This concern focuses on the possibility that older reactor vessels, embrittled by fast neutron irradiation, may be vulnerable to damage in certain severe overcooling transients in which the pressure remains relatively high. MSLB accidents have been identified as candidates for scrutiny in this regard.² The primary objective, then, was to predict primary-coolant pressure histories and vessel-wall temperature histories.

The first of the two cases incorporated fairly realistic assumptions regarding management of the feedwater and the emergency-core-cooling system (ECCS) following the MSLB. The feedwater supply was held constant at the steady-state flow rate for one minute, then decreased linearly to zero flow over the next two minutes. The ECCS flow was shut off when the pressurizer level recovered to its initial value. These actions represent a reasonable approximation to those that would be expected, either automatically or by operator intervention, in the event of an actual MSLB.

The predictions of Case 1 include a temporary blockage of natural circulation flow in the primary coolant system. However, the primary-coolant temperature transient was fairly moderate in the context of the pressurized-thermal-shock issue. Therefore, the second calculation incorporated assumptions designed to present a greater challenge to vessel integrity. The main feedwater was allowed to "runaway" at full flow for fifteen minutes, and the ECCS, once initiated, was left running indefinitely.

II. MODEL DESCRIPTION

Figure 1 shows a schematic diagram of the TRAC model used in the calculations. The finite difference noding is indicated on most components. The node numbers are helpful in the interpretation of some of the graphical results presented later.

For computational convenience, the two cold legs were combined in loop B (broken loop). However, they were modeled separately in loop A (intact loop) to allow for the possibility of a cold-leg break in other calculations utilizing the same input model. A TRAC steady-state calculation established an internally consistent set of initial conditions. A summary of these initial conditions is given in Table I.

The feedwater conditions required special modeling. The actual feedwater flow rate in B&W plants is about 772 kg/s, and the temperature is about 517 K, appreciably subcooled. This feedwater flow is introduced near the steam-generator midplane into a downcomer region where it is mixed with steam drawn into the downcomer by aspiration. As a result of this mixing, the secondary coolant enters the tube region at the bottom of the steam generator as saturated liquid. The TRAC steam-generator component does not permit direct modeling of the downcomer and aspirator flow. (A method to model them approximately in an indirect way with input modifications will be investigated in the near future.) In this study the feedwater was supplied directly to the bottom of the steam generator as saturated liquid and the actual flowrate was augmented by the quantity of steam needed to bring 772 kg/s of 517 K liquid to saturation. This should reproduce accurately the actual flowrate at the bottom of the steam generator, as well as provide the correct primary-to-secondary energy transfer in the steady-state calculation.

TABLE I
INITIAL CONDITIONS

Primary Coolant System

Reactor Power (MW)	2827
Pressure, pump inlet/discharge (MPa)	14.55/15.40
Hot leg temperature (K)	591
Cold leg temperature (K)	564
Core mass flowrate (kg/s)	1.74×10^4

Secondary Coolant System

Steam-generator inventory (kg)	2.163×10^4
Pressure, steam-generator outlet (MPa)	6.413
Steam temperature (K)	560.6
Feedwater temperature (K)	553.1
Feedwater flowrate (kg/s)	885.6

Numerous assumptions regarding system operation and control actions were incorporated into the calculations. Much of this information was specified by the Nuclear Regulatory Commission (NRC).³

- (1) The initiating event was the complete rupture of the 0.864-m-i.d. (34-in) main steam line in loop B at time = 0.0 s.
- (2) Initial reactor power was 2827 MW. It was held constant at this value until a low primary system pressure of 13.1 MPa (1900 psia) caused a reactor trip. After the reactor trip the power was dropped immediately to decay heat levels. Reactivity feedback was not modeled.

- (3) Both steam generators depressurized until the turbine isolation valves closed 0.5 s after reactor trip. Closure of these valves terminated the blowdown of the intact steam generator A.
- (4) Turbine bypass flow occurred when the secondary system pressure exceeded 6.55 MPa (950 psia). The capacity was assumed to be 40% of the normal steam flow, or 310 kg/s. Secondary-system safety valves also were modeled, but were not important in this calculation.
- (5) Auxiliary feedwater (AFW)
 - Case 1: Flow of 68 kg/s was initiated at $t = 30.0$ s. All AFW flow was aligned to the intact loop A generator.³
 - Case 2: AFW was assumed unavailable.
- (6) Main feedwater flowrate and temperature
 - Case 1: Constant volumetric flowrate of $1.138 \text{ m}^3/\text{s}$ for 60.0 s, then decreased linearly to zero over the next 120.0 s. The temperature was held constant at 553 K for 40.0 s, then decreased linearly to 326.0 K over the next 120.0 s. These feedwater conditions were imposed upon both steam generators.
 - Case 2: Constant volumetric flowrate of $1.138 \text{ m}^3/\text{s}$ for 900.0 s, then decreased linearly to zero over the next 120.0 s. The temperature was held constant at 553.0 K for 40.0 s, then decreased linearly to 305.5 K over the next 120.0 s. For case 2, a further condition was imposed upon the feedwater supply. It was assumed that the steam-driven main feedwater pumps were unavailable and that feedwater was supplied by other pumps present in the feedwater train. The characteristics of these pumps are unknown, but they have a shutoff head of approximately 3.45 MPa.³ Therefore, in cases 2 and 3, the feedwater flowrate was set to zero whenever the pressure in the steam-generator secondary exceeded this value. As will be seen, this resulted in shutoff of the feedwater to the intact steam generator soon after closure of the turbine stop valve.
- (7) The ECCS was started 35 s after the primary system pressure fell to 11.14 MPa. In Case 1, the ECCS was stopped when the pressurizer liquid level recovered to its initial value. In Case 2, the ECCS was allowed to run indefinitely.
- (8) The primary coolant pumps were tripped 15 s after ECCS initiation.

III. RESULTS

These transients are driven by the overcooling in the steam generators, initially caused by the blowdown of the original secondary-side water inventory, and later by the flashing of the feedwater. Therefore, examination of the steam generator response is given particular attention in the following discussion.

A. Case 1: (Rupture of steam line B at $t = 0.0$ s. Feedwater flow continued to both generators for 3 minutes. All auxiliary feedwater aligned to intact generator A. HPI terminated with pressurizer level recovery.)

The early part of this transient is dominated by the blowdown of steam generator B. The steam-line break caused rapid voiding and depressurization of the secondary side. As a consequence of the initial blowdown and also the flashing of the feedwater, there was substantial cooling of the primary-side liquid during the first three minutes of the transient (Fig. 2). After three minutes, when the main feedwater was completely shut off, both primary and secondary fluids were essentially stagnant, and steam generator B had little effect upon the rest of the transient.

Attention now will be directed to steam generator A, with reference to Figs. 3-9. Although the steam line remained intact in loop A, it was assumed that there was direct communication with the break in loop B until the turbine isolation valves were closed at 8.3 s. Therefore, steam generator A also experienced blowdown during this time and nearly completely voided as shown in Fig. 3. After closure of the valve however, the main feedwater flow quickly refilled the generator entirely full of liquid at about 100 s (Fig. 3).

Figure 4 shows that after isolation of the steam generator, the secondary rapidly repressurized to the set point of the turbine bypass system, 6.55 MPa (950 psia), and held at this pressure, with a corresponding saturation temperature of 555 K. At about 50 s, the overcooling of the primary by the continued blowdown in loop B produced a primary inlet temperature to the loop-A steam generator lower than 555 K. Consequently, the steam in the upper portion of the secondary cooled, and the pressure fell, as shown in Fig. 4. This trend continued until the secondary was filled completely with liquid at about 110 s. The subsequent pressure decrease, seen in Fig. 4 from about 110 s to about 420 s, occurred during the filling of the steam line with liquid. Condensation of the pre-existing vapor accounted for the pressure behavior. The steam line finally filled at about 420 s, causing a rapid increase in pressure until equilibrium was established at about 6.7 MPa by opening of some of the safety valves.

Figure 5 shows the coolant mass flow rate on the primary side of the intact-loop steam generator. The coolant flow was blocked completely from 110 s until 230 s. This situation arose in the following way. The overcooling of the primary coolant system by the blowdown of the steam generators, especially the longer blowdown of generator B, produced shrinkage of the coolant volume at a rate greater than could be compensated by ECC flow. The pressurizer emptied and a substantial void fraction developed in loop A. (The continued blowdown of the loop-B generator produced subcooling of the primary coolant in the loop. Only loop A reached saturation.) While the pumps were running, the coolant void was distributed around the loop in a two-phase mixture. However, after the pump trip at 60 s and the subsequent coastdown, phase separation occurred, with vapor collecting at the higher elevations of the loop, namely the hot-leg candy cane

and the upper portion of the steam generator, Figs. 6 and 7. This blocked natural convection flow.

The eventual removal of the flow blockage apparently was caused by condensation of the steam in the upper portion of the steam-generator primary. Careful comparison of Figs. 6 and 7 shows that the void collapse in the steam generator precedes that in the candy cane. The condensation in the steam generator began at about 100 s when the secondary side filled with liquid (Fig. 4) and the cold auxiliary feedwater caused significant primary-to-secondary energy removal at the top of the steam generator. The resulting vacuum drew relatively cold liquid around the loop, eventually removing the void.

Figure 8 shows the secondary coolant temperature for the five computational cells in steam generator A. Cell 1 received the main feedwater flow and therefore was influenced most strongly by the feedwater temperature. The temperature in nodes 2 and 3 also followed the decreasing feedwater temperature, but less closely than node 1 because of heat transfer from the primary side. Node 5 contained the inlet for the auxiliary feedwater. Thus, the fluid temperature of node 5 differed significantly from that of node 4 after 100 s when the secondary side filled with liquid. After re-establishment of flow on the primary side at about 235 s, the lower four cells of the now stagnant secondary coolant eventually equilibrated at about 478 K, and then all energy removal from the system was accomplished by the auxiliary feedwater in node 5.

Figure 9 shows related temperature data for the seven nodes of the primary coolant in steam generator A. Early in the transient, from about 40 s to about 90 s, the primary coolant was saturated. Therefore, there was little temperature variation with position during this period; any heat transfer

produced vaporization or condensation. However, after stagnation of the primary flow at about 100 s, a considerable spatial temperature distribution developed. Node 2 was exposed directly to the feedwater flow and cooled rapidly until the feedwater flow stopped at 180 s. The liquid temperature in this node rapidly increased after the primary flow started again at 235 s. At later times in the transient, nodes 1 through 6 were all at virtually the same temperature, reflecting the absence of main feedwater flow. As noted above, all energy removal from the system late in the transient was by the auxiliary feedwater, and correspondingly, the only significant temperature variation in the steam-generator primary coolant temperature took place between nodes 6 and 7 as shown on Fig. 9.

The important aspects of the behavior of steam generator A can be summarized as follows. During the first 8 s, the secondary side nearly emptied of liquid because of communication with the assumed steam line break in loop B. After closure of the turbine isolation valve, the secondary side repressurized and refilled with liquid. Meanwhile, the overcooling of the primary by the continued blowdown in loop B resulted in shrinkage of the primary coolant volume and the evolution of a significant void fraction that was distributed as a two-phase mixture in loop A. After the trip and coastdown of the primary coolant pumps, the phases separated, with a resultant "vapor lock" in the high elevations of loop A temporarily blocking primary coolant flow. The vapor condensed after about 235 s, natural convection coolant flow was established, and eventually the system energy was removed by the loop A auxiliary feedwater.

Additional results of interest are given in Figs. 10-13. Figure 10 shows the primary system pressure history. After 300 s, the pressure stabilized at about 3 MPa (435 psia). Figure 11 gives the ECCS mass flow rate for loop B

(negative values imply flow into the system). Each of the two ECCS flow rates in loop A were one half the values in Fig. 11. The ECCS flow was terminated when the pressurizer liquid level recovered to its initial value, which occurred at about 700 s (see Fig. 12). There was no core uncover in this transient, and the average fuel rod temperature dropped about 100 K from the initial steady-state operating value.

The most important parameters relevant to pressurized thermal shock are the primary coolant system pressure (Fig. 10) and the primary coolant temperature. Figure 13 shows the liquid temperature at the top of the downcomer, the coldest fluid to which the vessel is exposed. The solid line gives the temperatures at an azimuthal vessel location associated with the broken-loop side of the vessel, whereas the dashed line corresponds to the intact-loop side. The asymmetrical cooling in the two loops is reflected.

B. Case 2: (Rupture of steam line B at $t = 0.0$ s. Feedwater flow continued to both generators for 15 minutes. Auxilliary feedwater unavailable. HPI not terminated.)

The secondary side of the loop B steam generator (the loop with the MSLB) again quickly emptied of liquid because of the rapid blowdown following the steam-line break at time zero. However, because full feedwater flow was maintained in this case, the generator was refilled again with liquid at about 300 s (Fig. 14). The depressurization of the secondary side of steam generator B is shown in Fig. 15. Just as in case 1, there was no voiding in loop B. This is because the overcooling by the blowdown of the steam generator and the flashing of the continuing feedwater kept the primary coolant in this loop well subcooled. The voiding produced by volumetric shrinkage of the primary liquid again appeared in the hotter intact loop A, as will be seen shortly. Feedwater

was supplied to the intact steam generator A only for the first few seconds of the transient. The flow shut off when the pressure in the secondary side of the steam generator recovered to 3.45 MPa (see earlier discussion in section II). Figure 16 shows this to have occurred very early in the transient, soon after closure of the turbine stop valve isolated the steam generator. Figure 17 shows that the intact steam generator almost completely emptied during the initial blowdown, similar to Case 1. In this transient however, because the feedwater was terminated very soon thereafter, the loop A generator remained nearly empty throughout the calculation.

This calculation again showed void formation in the high elevations of the intact primary loop (Fig. 18) with consequent blockage of natural convection flow (Fig. 19) after coastdown of the primary coolant pumps. In this case however, with no feedwater supplied to the intact steam generator, there was no mechanism for relatively early removal of the flow blockage as in Case 1. The candy-cane void remained until late in the transient (about 1400 s) when the high-pressure injection flow finally refilled the system and caused abrupt pressure recovery (Fig. 20).

The primary-coolant-system pressure history of Fig. 20 exhibits interesting features. After the initial rapid depressurization driven by blowdown of the steam generators, especially the broken-loop generator with continuing feedwater, there was a pressure "plateau" from about 180 s until almost 600 s. This was caused by the stagnant vapor in the high elevations of the intact loop. At about 300 s, a small flow of relatively cool water started in the intact loop. This is attributable to the filling of the broken loop steam generator, Fig. 14. The consequent reduction of overcooling and volumetric shrinkage rate in the broken loop made a small flow available to the intact loop. At about

600 s, the pressurizer started to fill (Fig. 21). The pressure decrease between roughly 600 s and 800 s on Fig. 20 correlates closely with the filling of the pressurizer and apparently was driven by condensation. This may be due to the coarse noding in the pressurizer component. After the pressurizer filled, the primary pressure was again nearly constant until the final repressurization, when the remaining voids were removed. Figure 22 shows the liquid temperature at the top of the downcomer, again with some azimuthal variation.

IV. SUMMARY AND CONCLUSIONS

The two MSLB calculations differ primarily in the assumed management of the feedwater supply to the steam generators. Case 1 represents the most likely sequence, with the main feedwater supply shut off early and all auxiliary feedwater aligned to the intact loop. One interesting feature of this calculation is the prediction of a temporary primary-coolant flow blockage to the intact steam generator, the only available heat sink. The blockage ultimately was removed by condensation driven by the AFW. The minimum vessel coolant temperature was about 420 K at about 200 s (Fig. 13) with a corresponding primary pressure of about 3 MPa (Fig. 10).

Case 2 represents a more severe overcooling transient because the main feedwater supply was assumed to "runaway" at full steady-state flow rate for 15 m. The minimum coolant temperature in this case was about 325 K, again with a pressure of about 3 MPa.

Figures 10, 13, 20, and 22 show for these cases the important variables from the standpoint of the pressurized thermal shock issue, namely the primary-coolant pressure and minimum temperature.

REFERENCES

1. R. C. Kryter, R. D. Cheverton, F.B.K. Kam, T. J. Burns, R. A. Hedrick, C. W. Moyo, "Evaluation of Pressurized Thermal Shock", NUREG/CR-2083, ORNL/TM-8072, Oak Ridge National Laboratory, (October 1981).
2. Safety Code Development Group, "TRAC-PD2 An Advanced Best Estimate Computer Program for Pressurized Water Reactor Loss-of-Coolant Accident Analysis," Los Alamos National Laboratory report LA-8709-MS (May 1981).
3. L. S. Shotkin, USNRC, personal communication.

LIST OF FIGURES

- Fig. 1. Schematic diagram of TRAC model.
- Fig. 2. Case 1 broken loop OTSG primary-side liquid temperatures for seven computational cells shown on Fig. 1.
- Fig. 3. Case 1 intact loop OTSG secondary-side water level.
- Fig. 4. Case 1 intact loop OTSG secondary-side pressure.
- Fig. 5. Case 1 intact loop OTSG primary-side mass flow rate.
- Fig. 6. Case 1 void fraction at top of intact-loop hot leg.
- Fig. 7. Case 1 intact loop OTSG primary-side void fraction for the five computational cells shown on Fig. 1.
- Fig. 8. Case 1 intact-loop OTSG secondary-side liquid temperatures for the five computational cells shown on Fig. 1.
- Fig. 9. Case 1 intact-loop OTSG primary-side liquid temperatures for the seven computational cells shown on Fig. 1.
- Fig. 10. Case 1 primary-system pressure.
- Fig. 11. Case 1 loop B ECCS mass flowrate.
- Fig. 12. Case 1 pressurizer water level.
- Fig. 13. Case 1 liquid temperature at top of vessel downcomer.

Fig. 14. Case 2 broken-loop OTSG secondary-side water level.

Fig. 15. Case 2 broken-loop OTSG secondary-side pressure.

Fig. 16. Case 2 intact-loop OTSG secondary-side pressure.

Fig. 17. Case 2 intact-loop OTSG secondary-side water level.

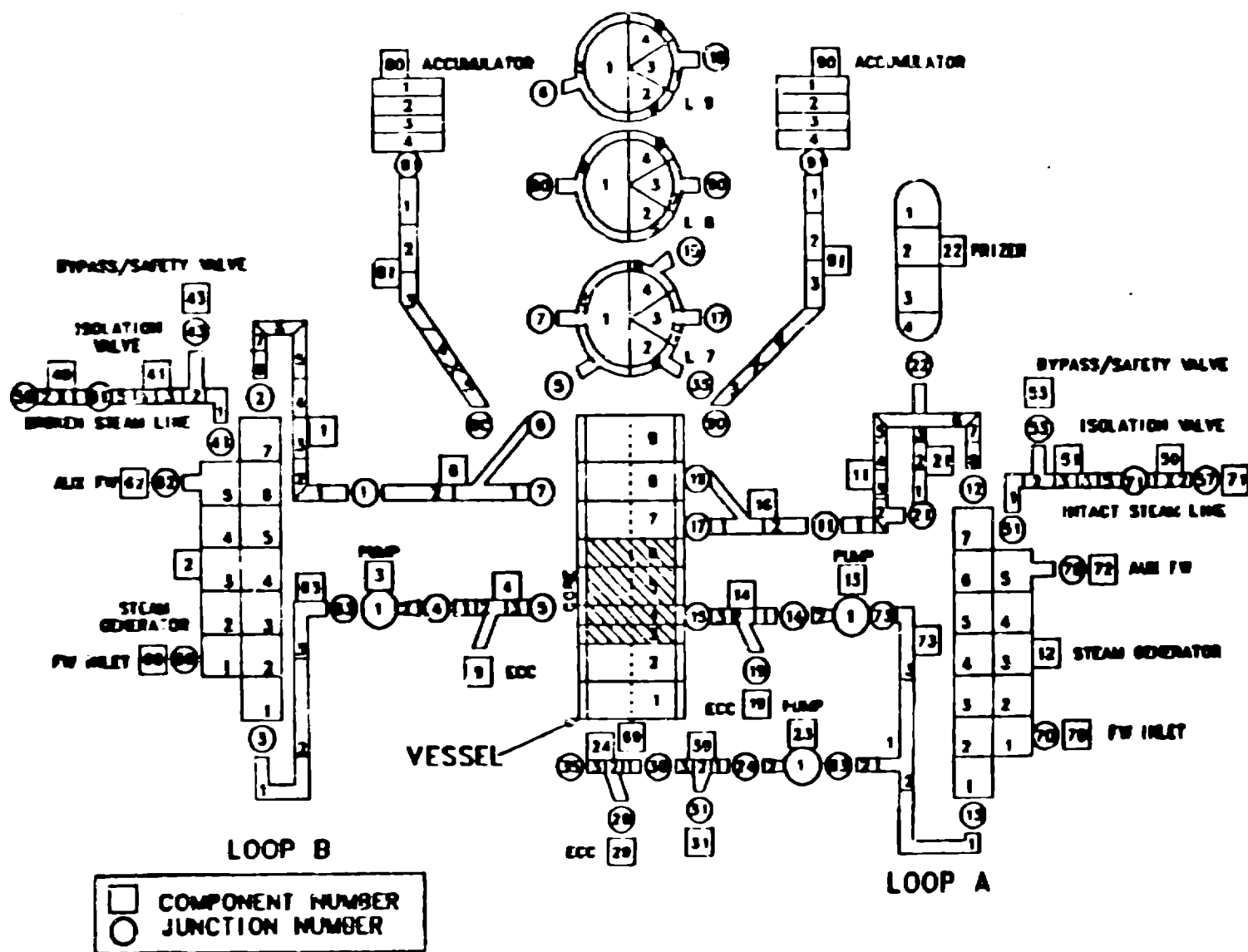
Fig. 18. Case 2 void fraction at top of intact-loop hot leg "candy cane."

Fig. 19. Case 2 intact-loop hot-leg coolant mass flowrate.

Fig. 20. Case 2 primary-coolant-system pressure.

Fig. 21. Case 2 pressurizer water level.

Fig. 22. Case 2 liquid temperature at top of downcomer.



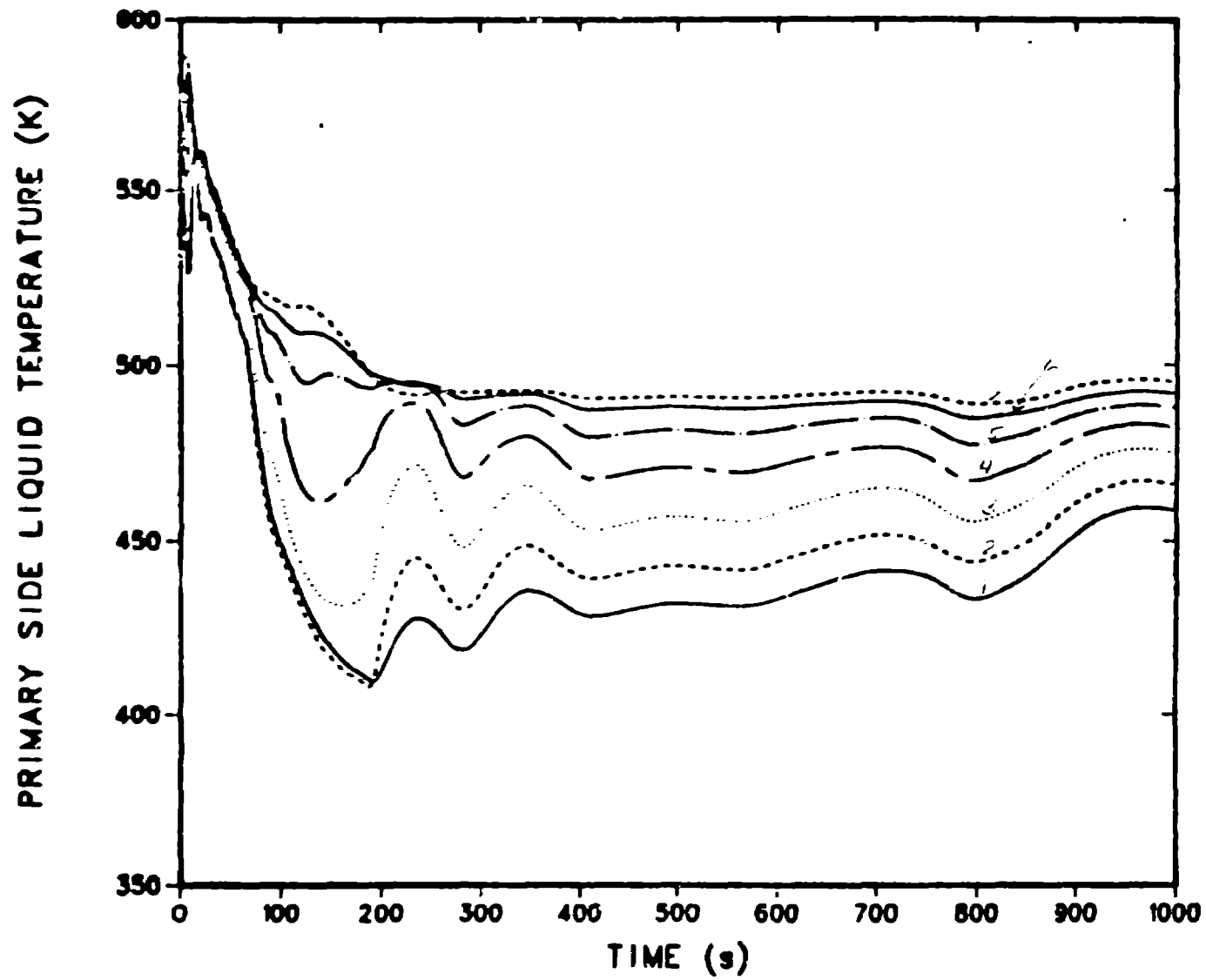
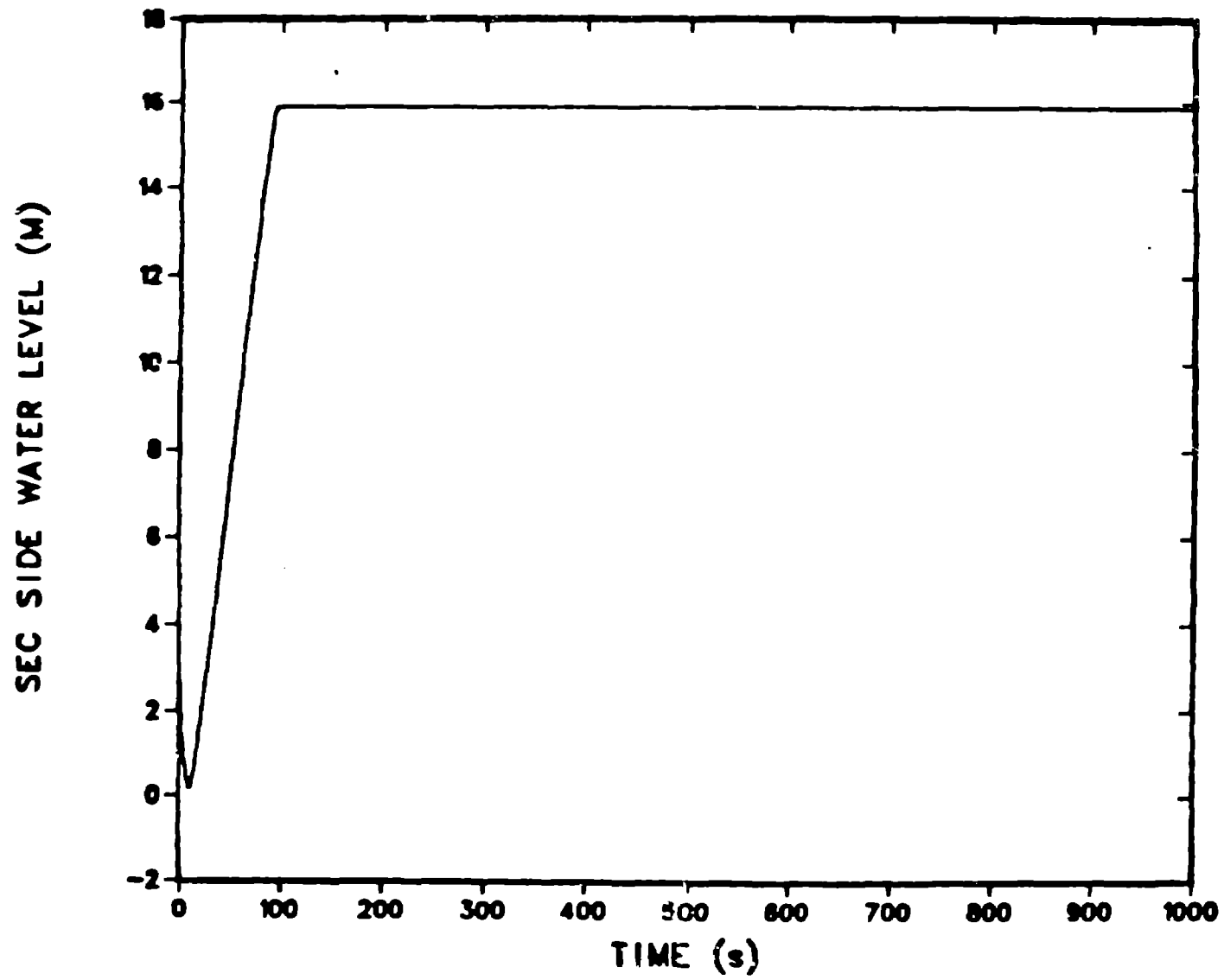


Fig. 2

OCTMI MSLB
INTACT LOOP OTSG SECONDARY SIDE WATER LEVEL



5.1

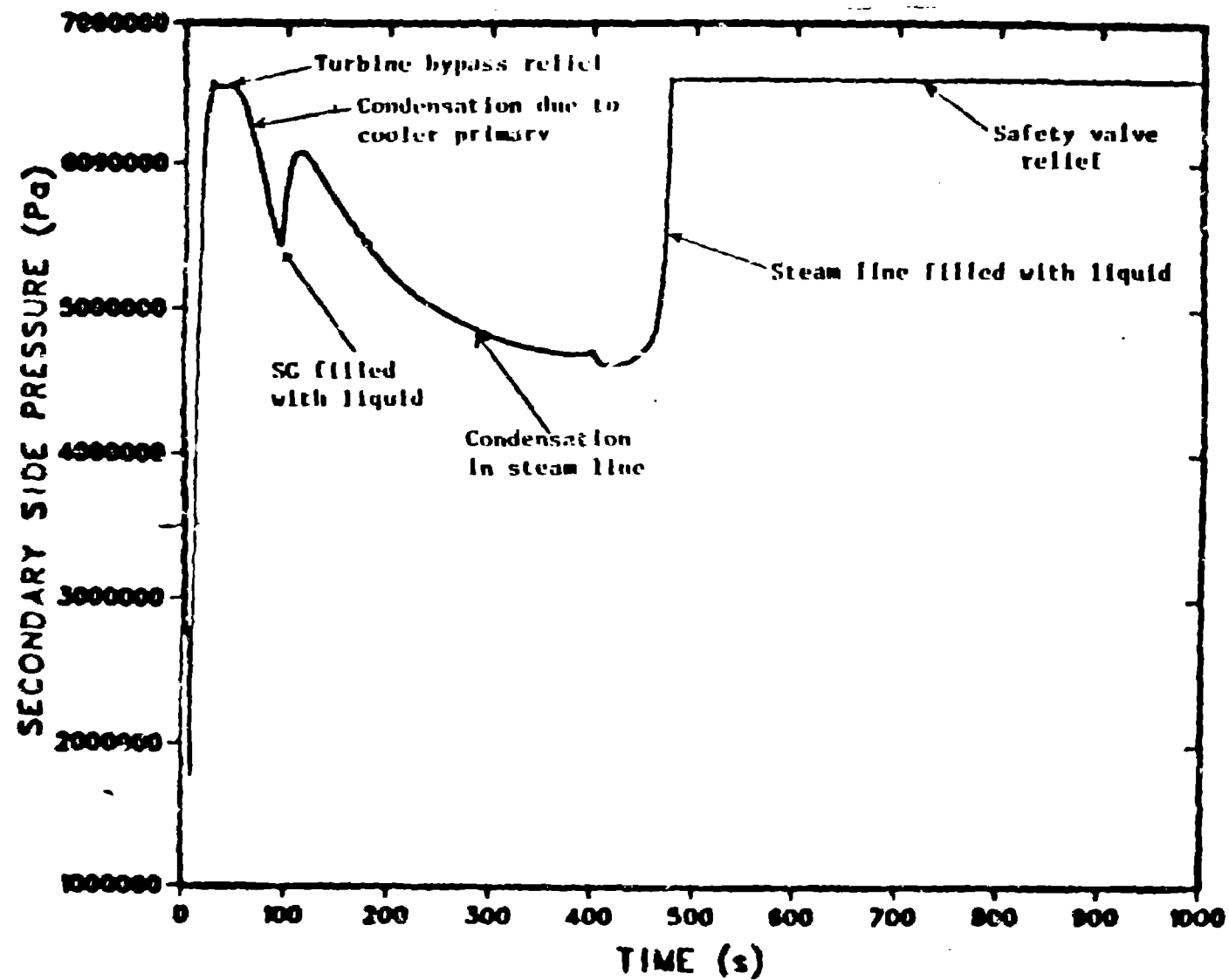
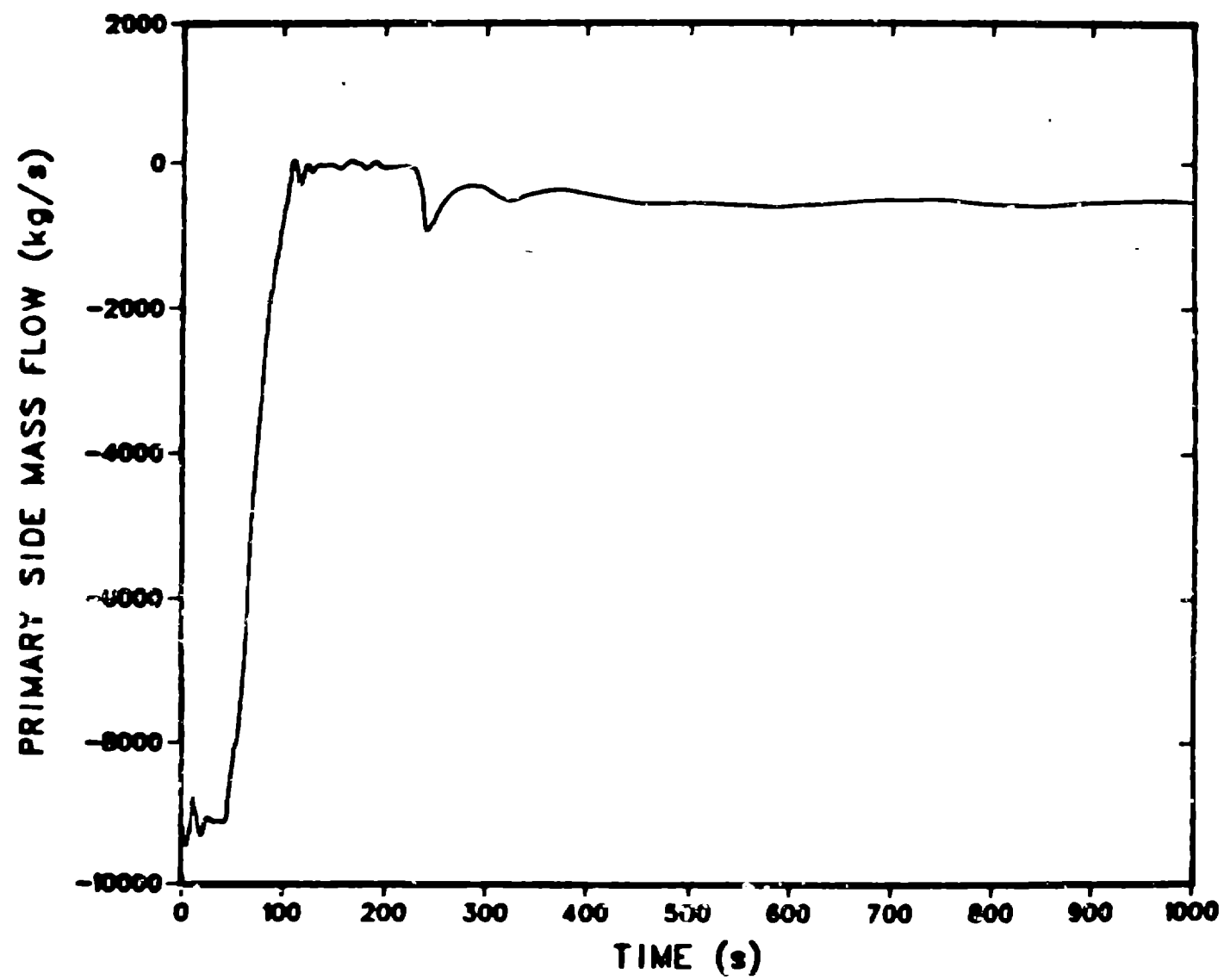


Fig 4



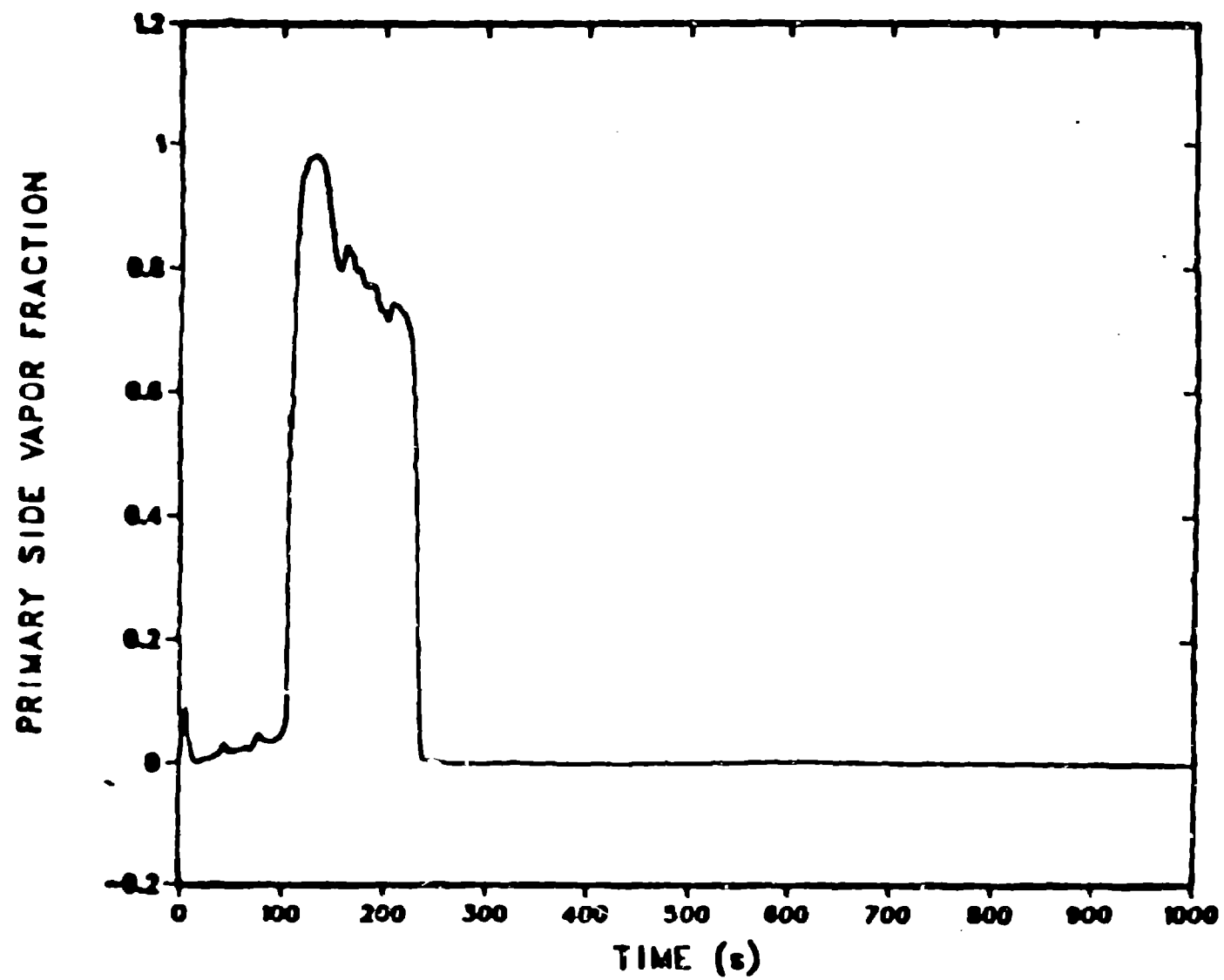


Fig. 6

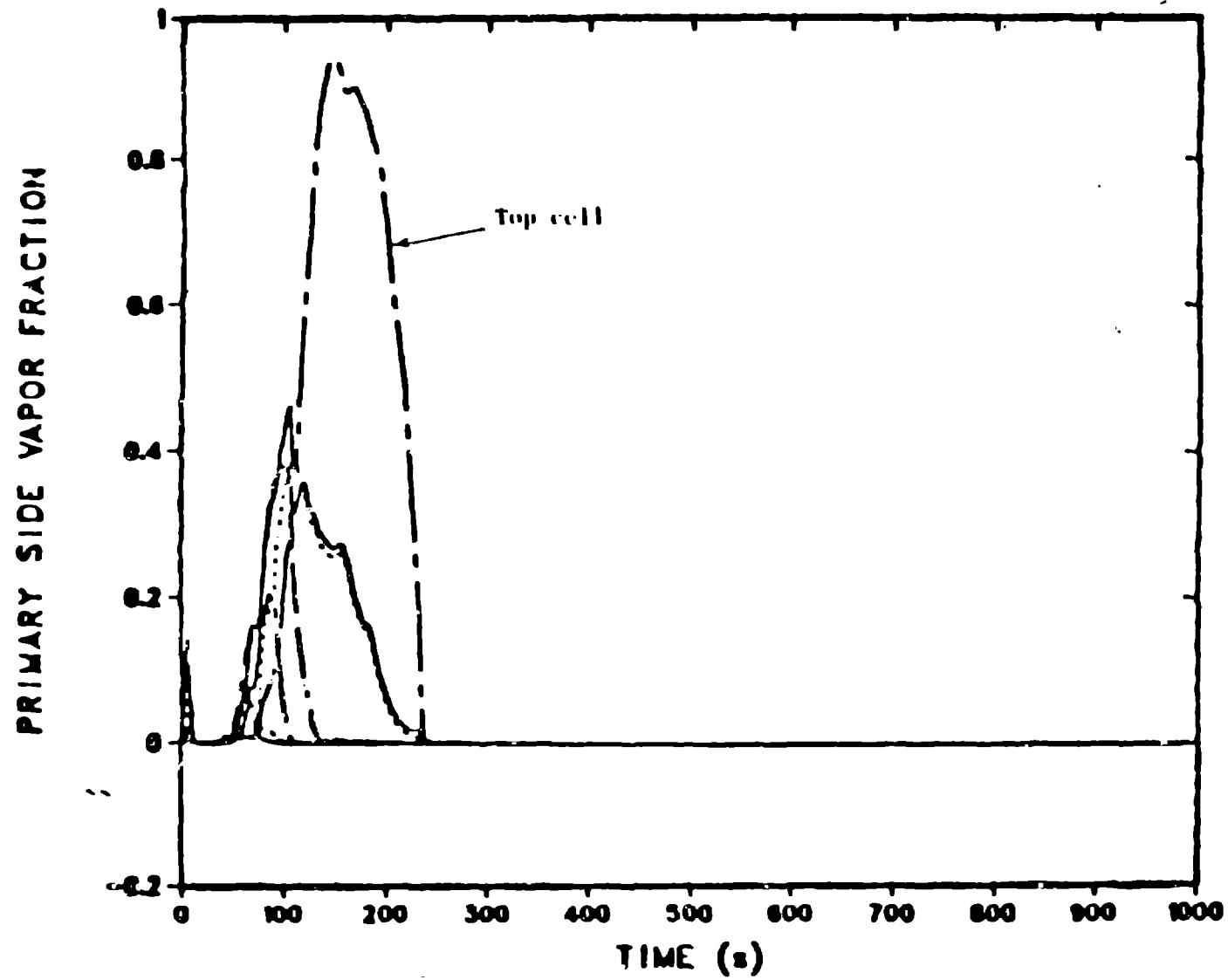
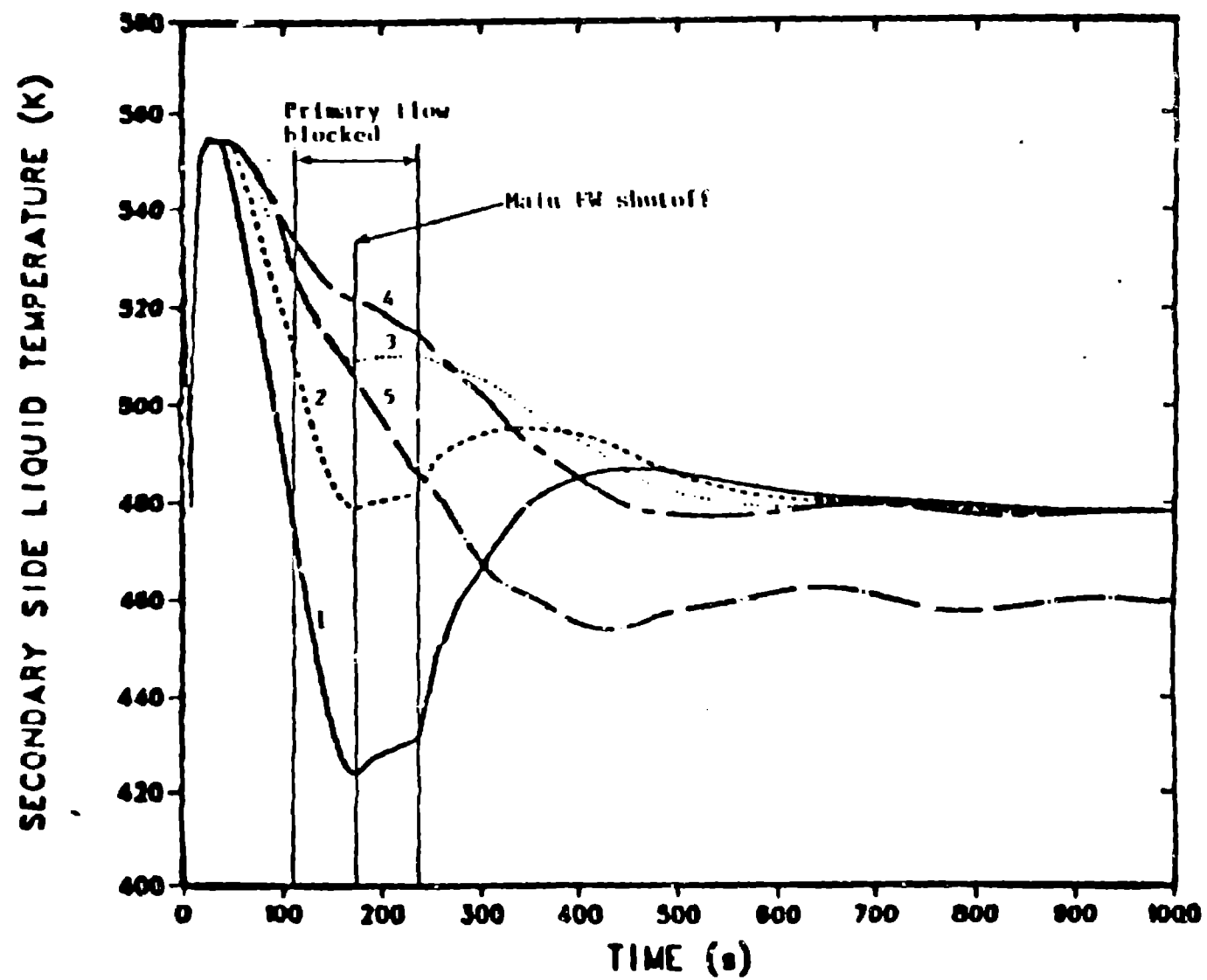
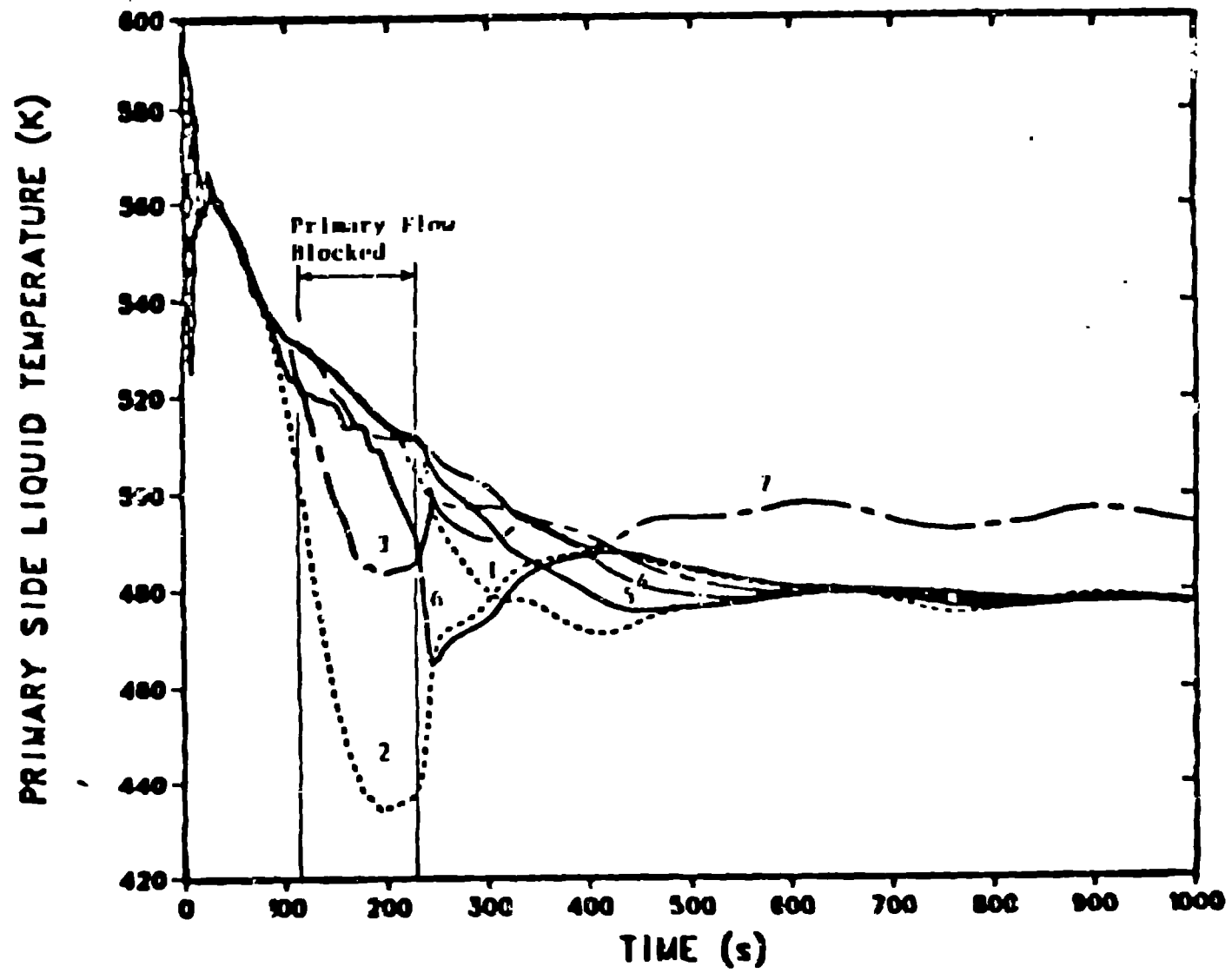


Fig. 1





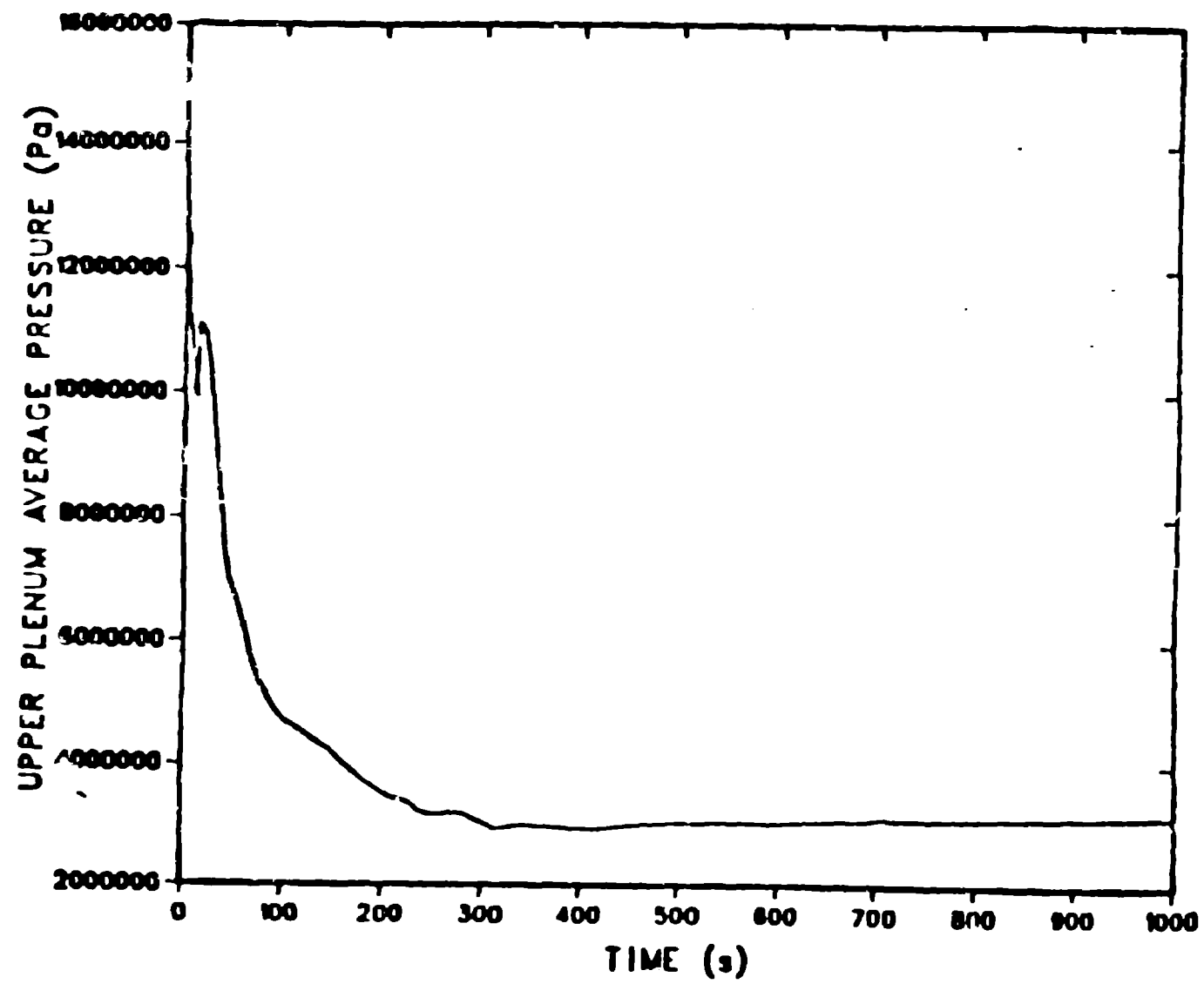
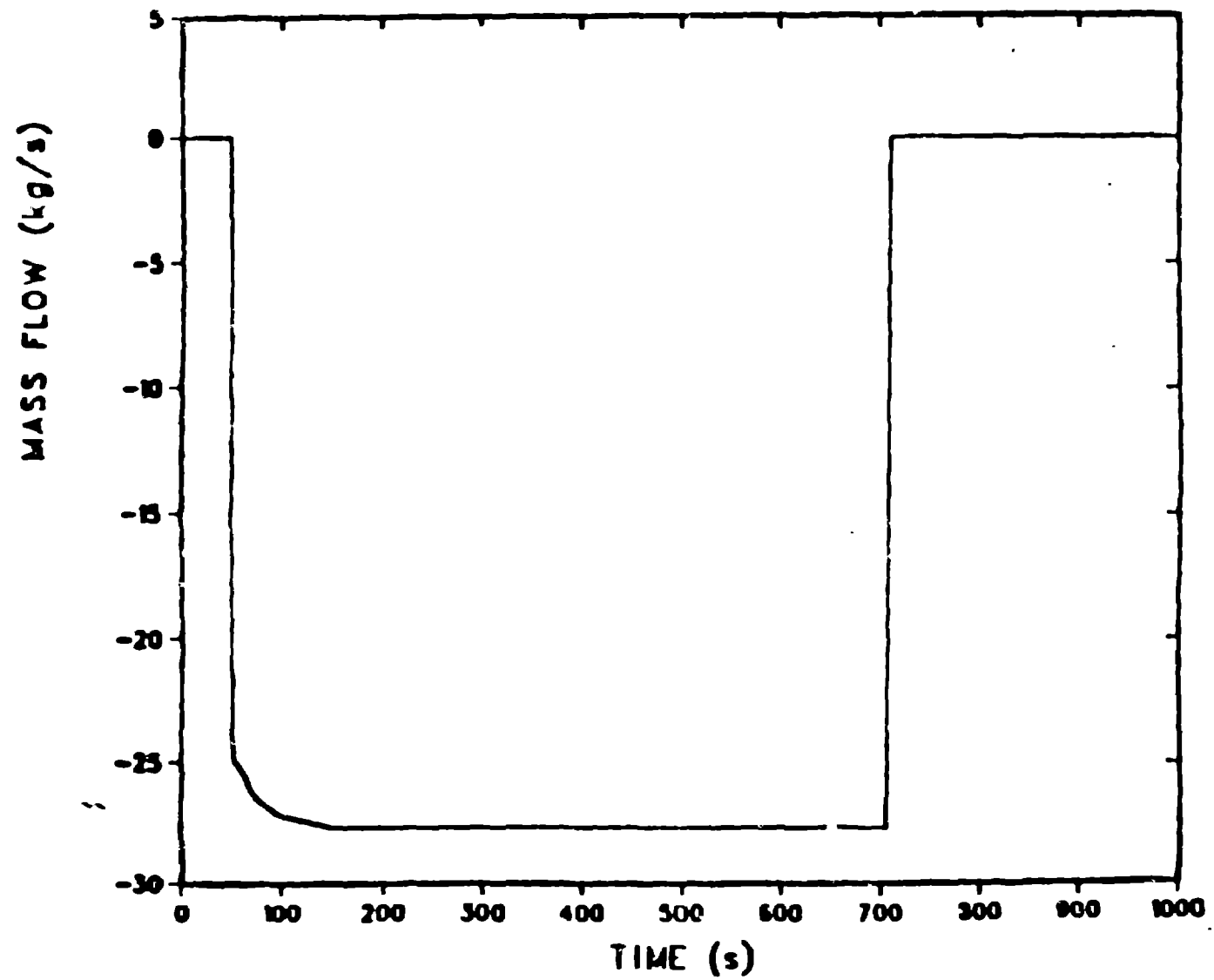


Fig. 10



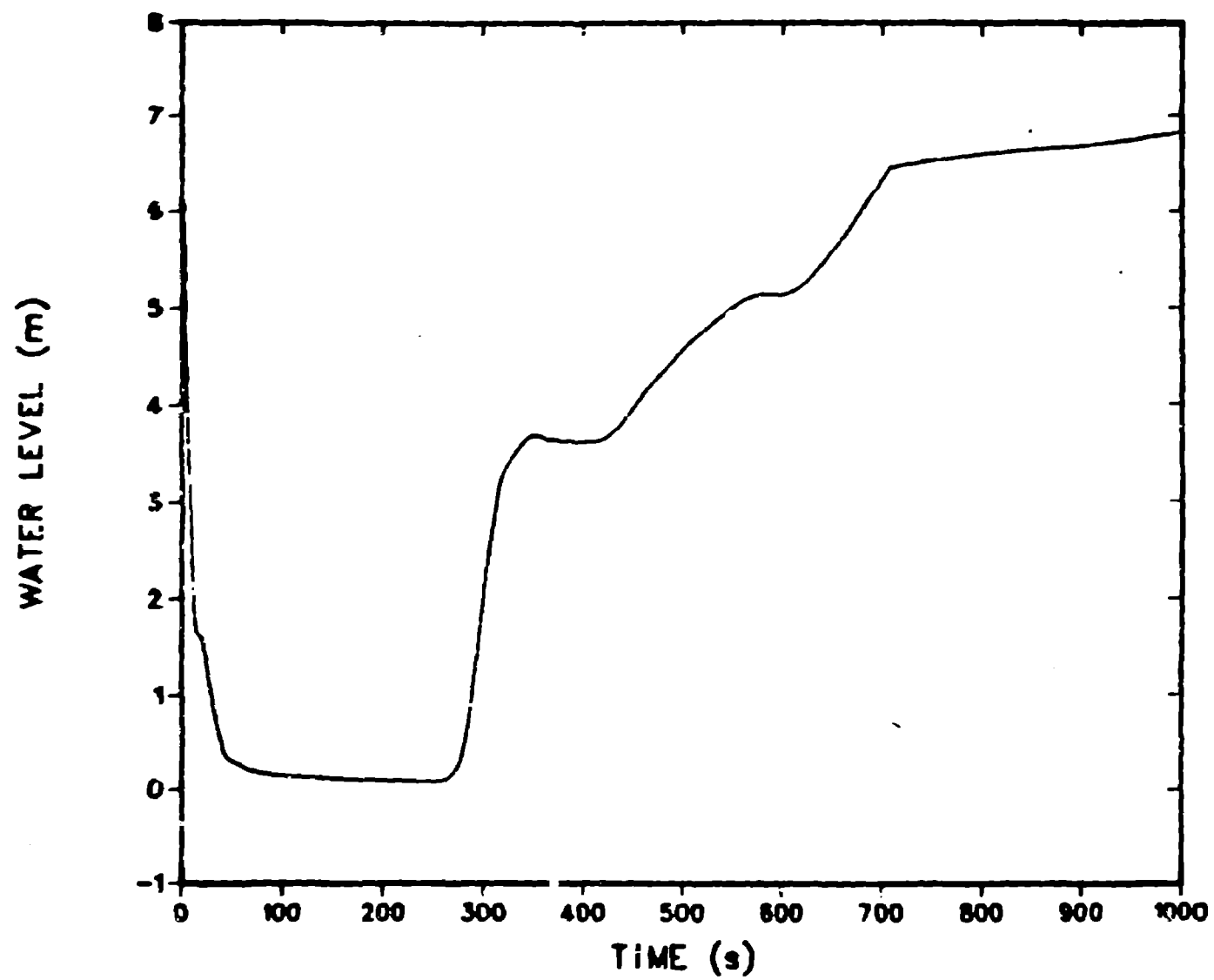
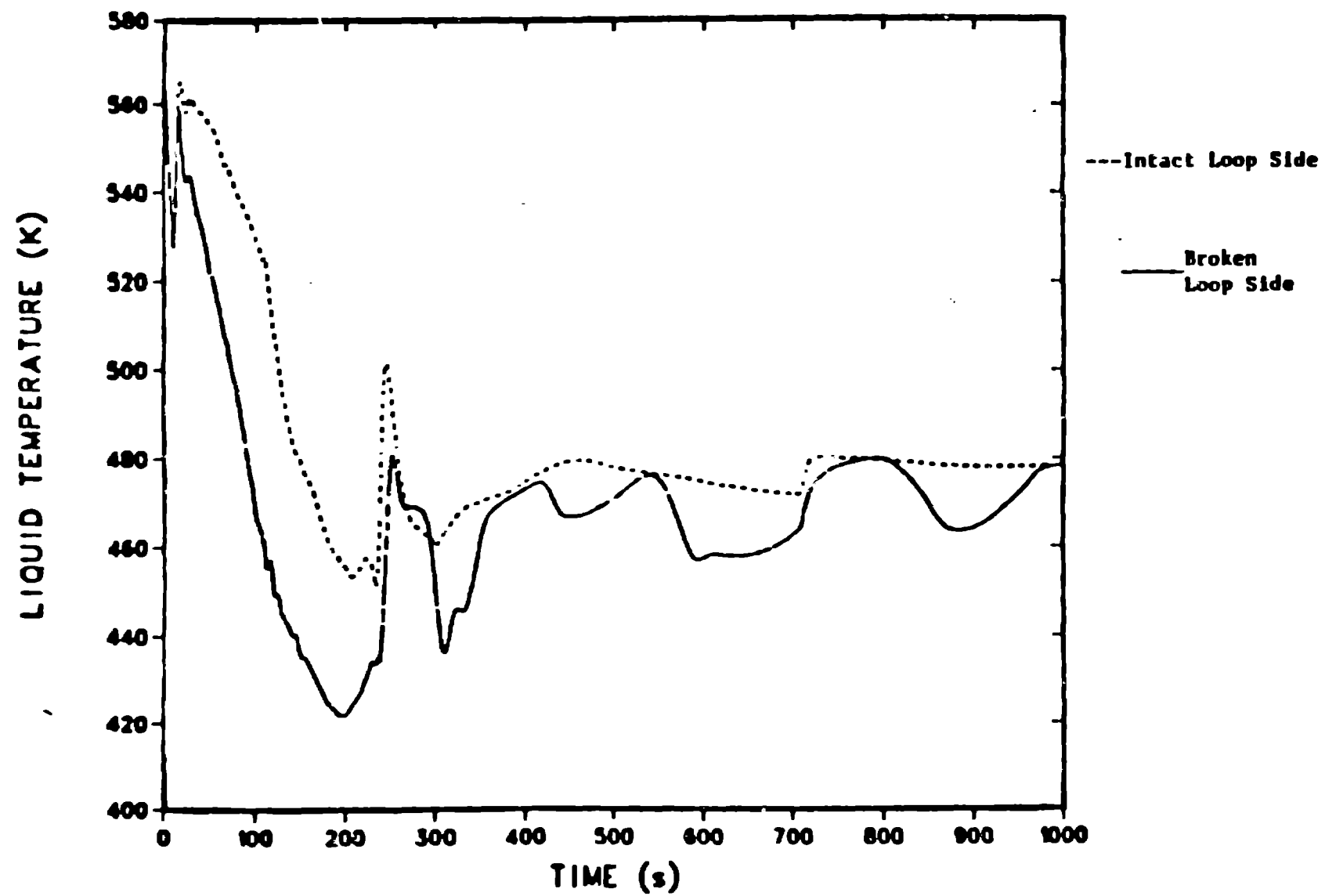
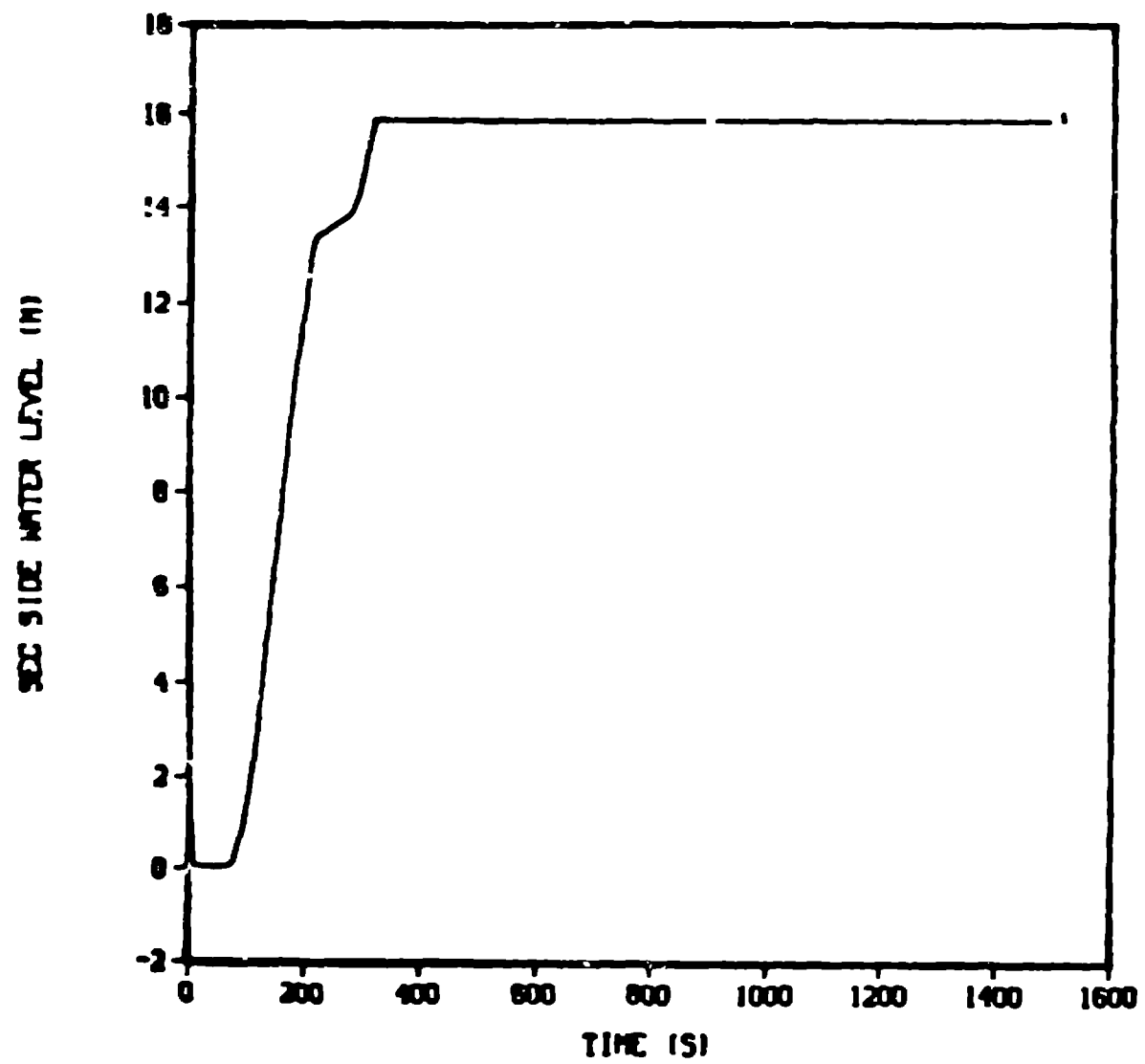


Fig. 12

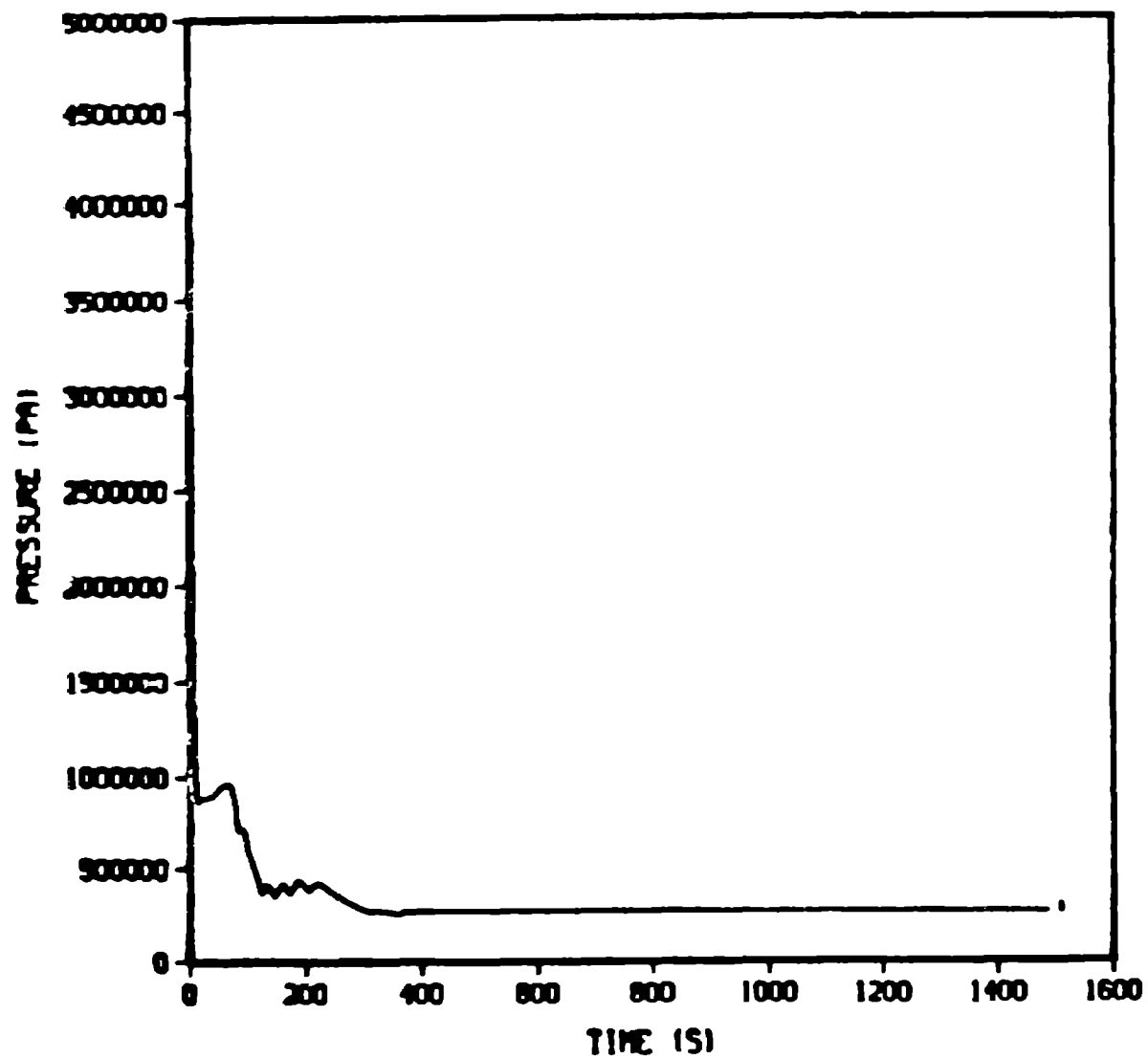




CELL
1

STGEN
SECONDARY
10 - 2

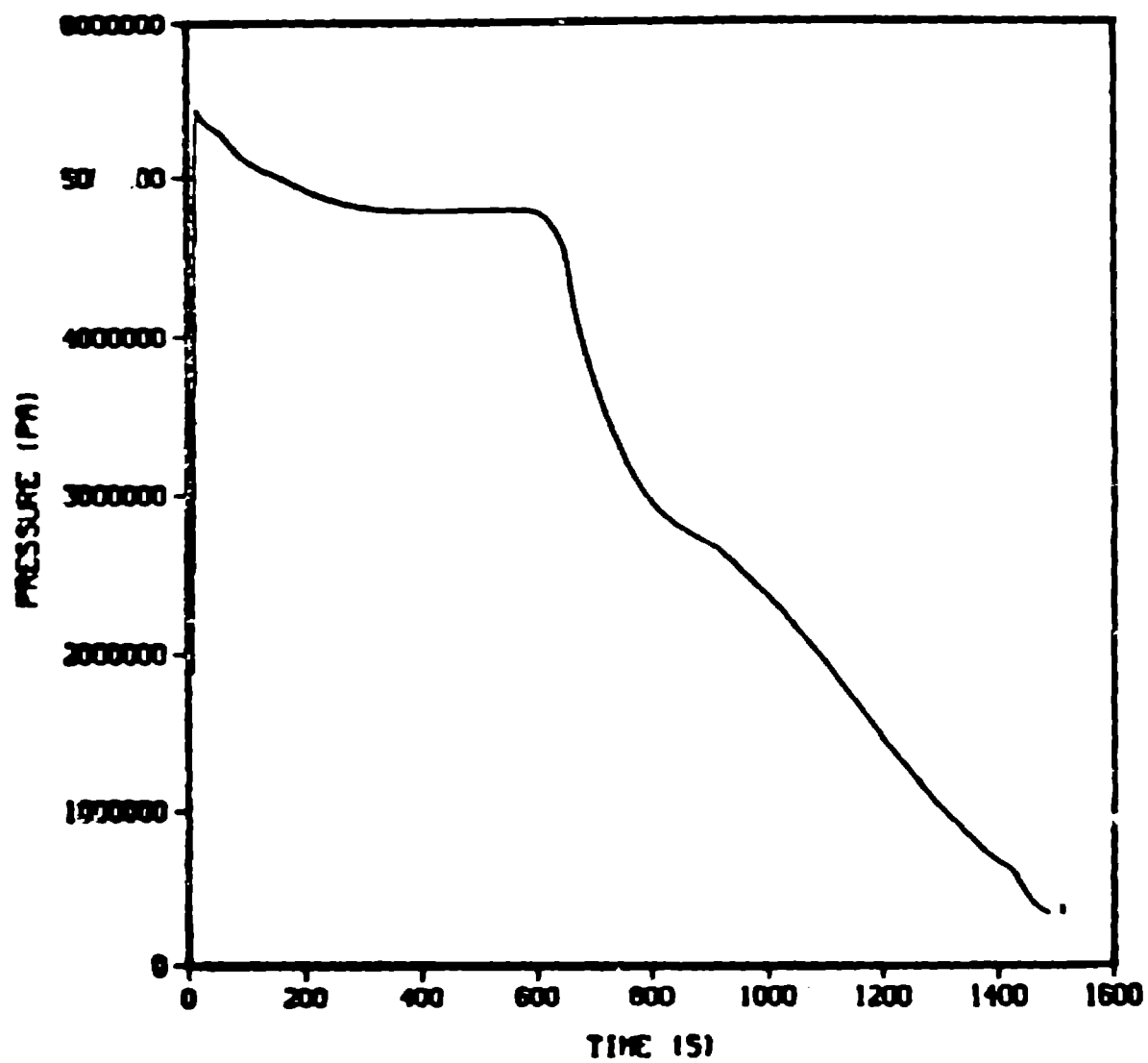
Aug 11/11



CELL
1

STGEN
SECONDARY
10 - 2

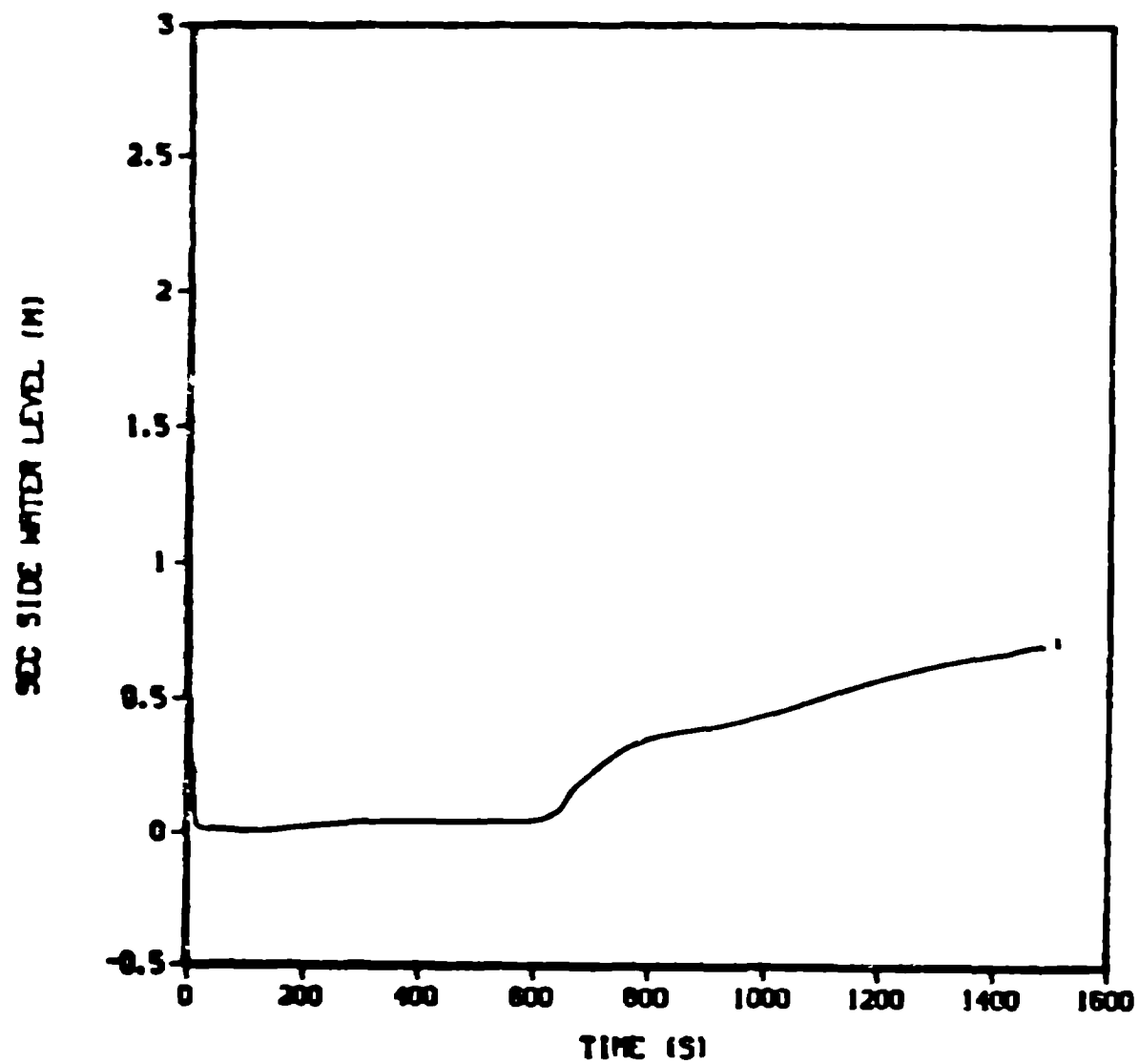
Fig. 15



CELL
1

STGEN
SECONDARY
10 - 12

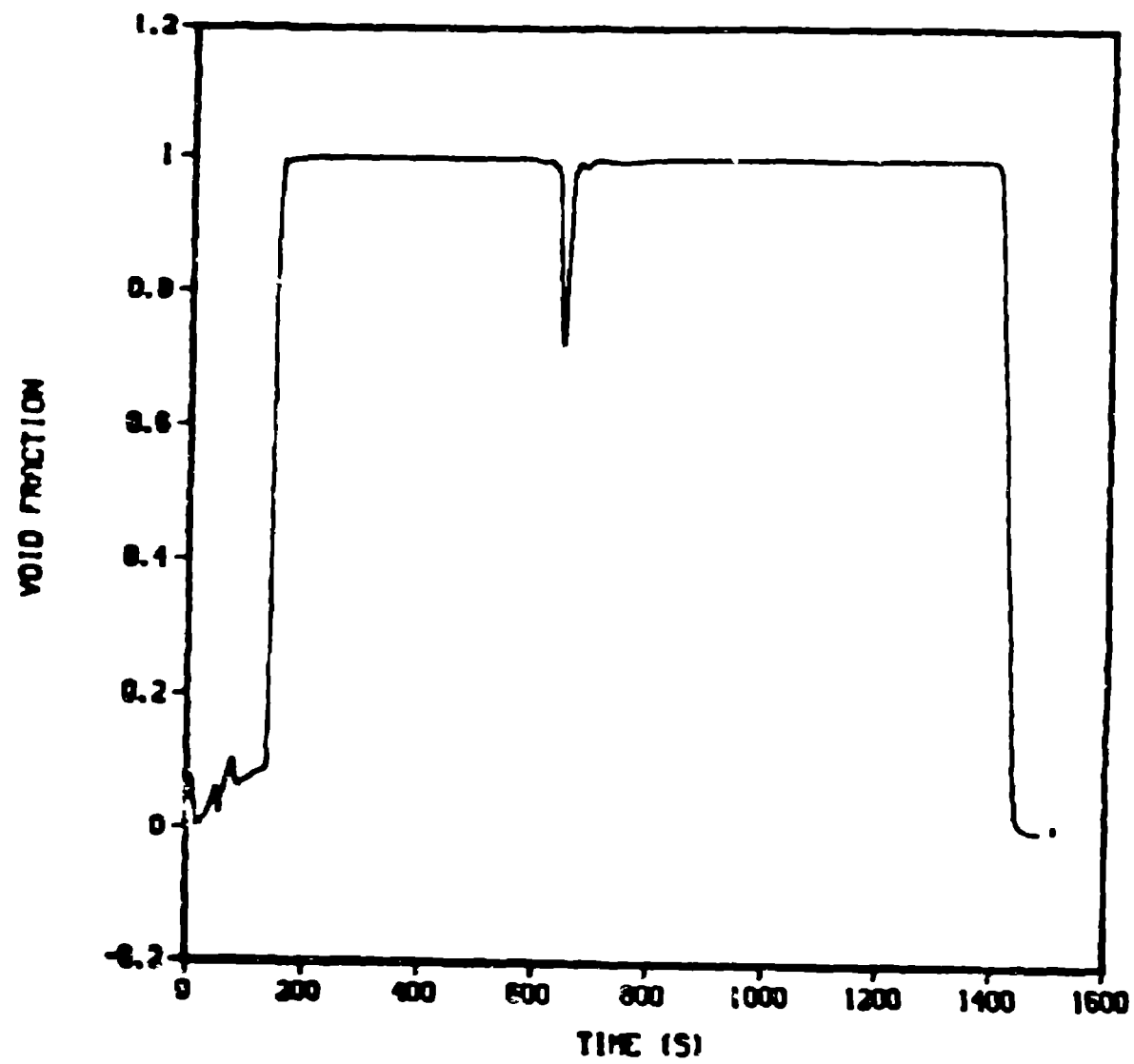
Fig. 10



CELL
1

STGEN
SECONDARY
10 - 12

4.1.1

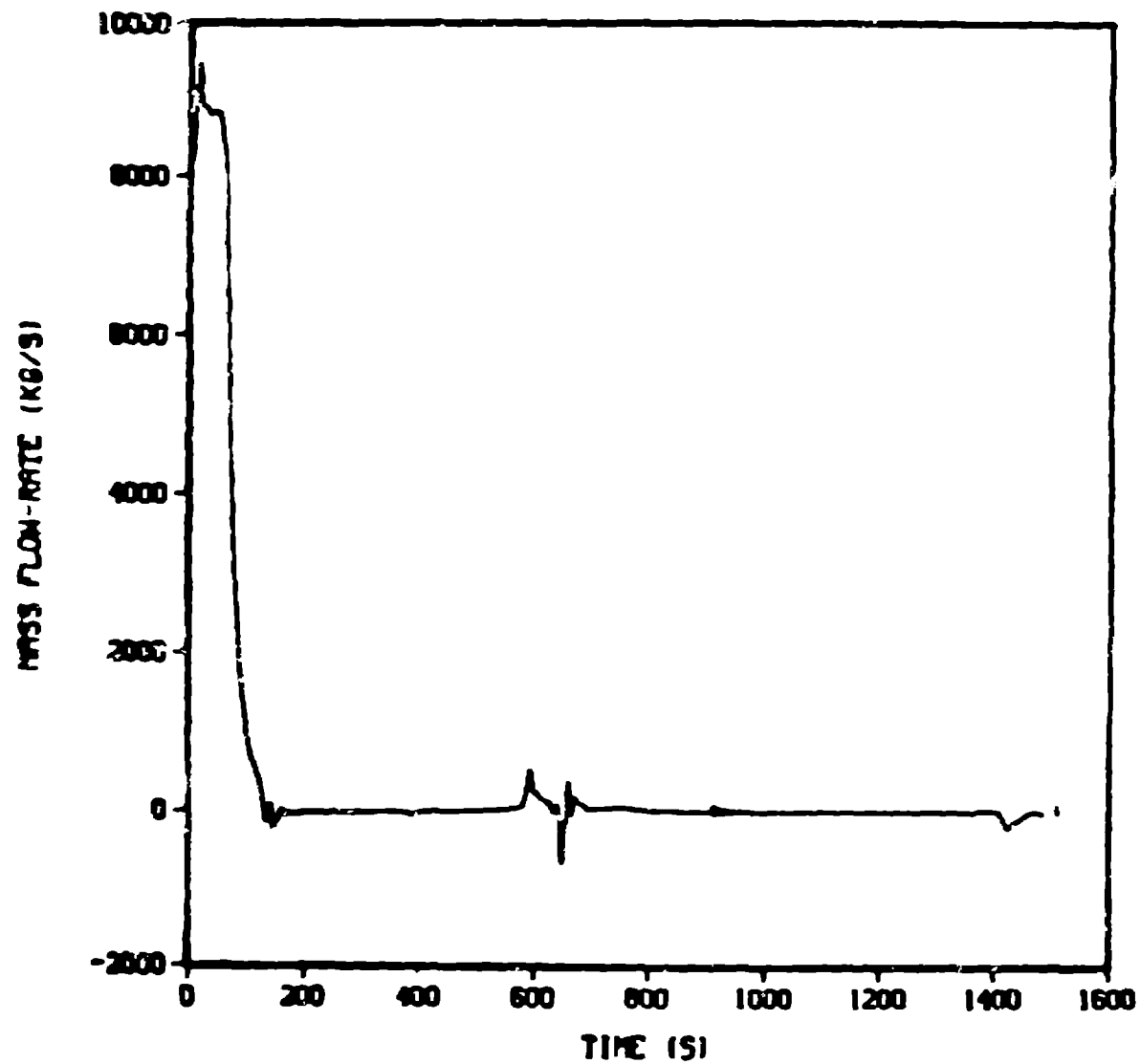


CELL
6

TEE
PRIMARY
ID - 11

1

Fig. 18

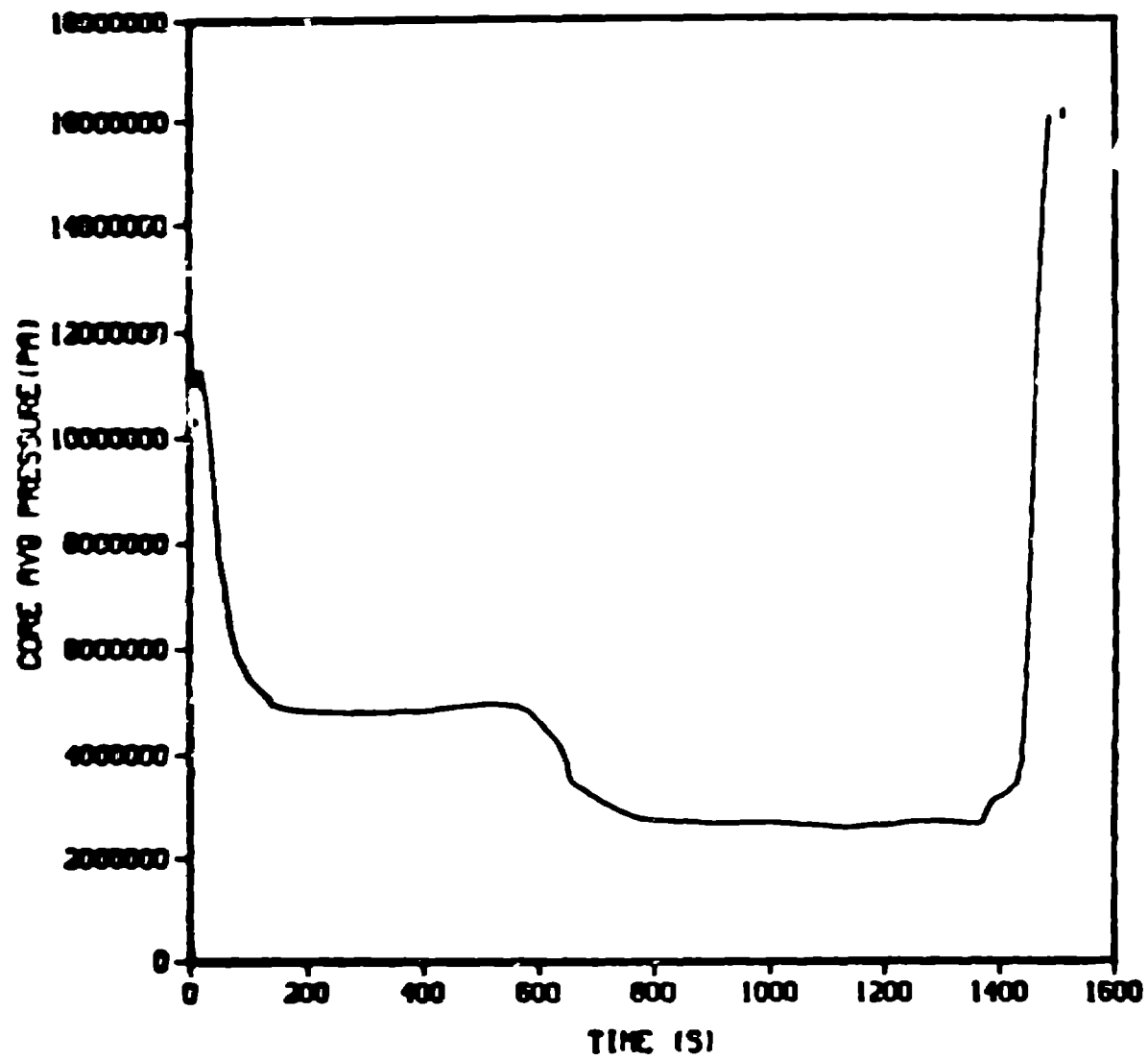


CELL

2

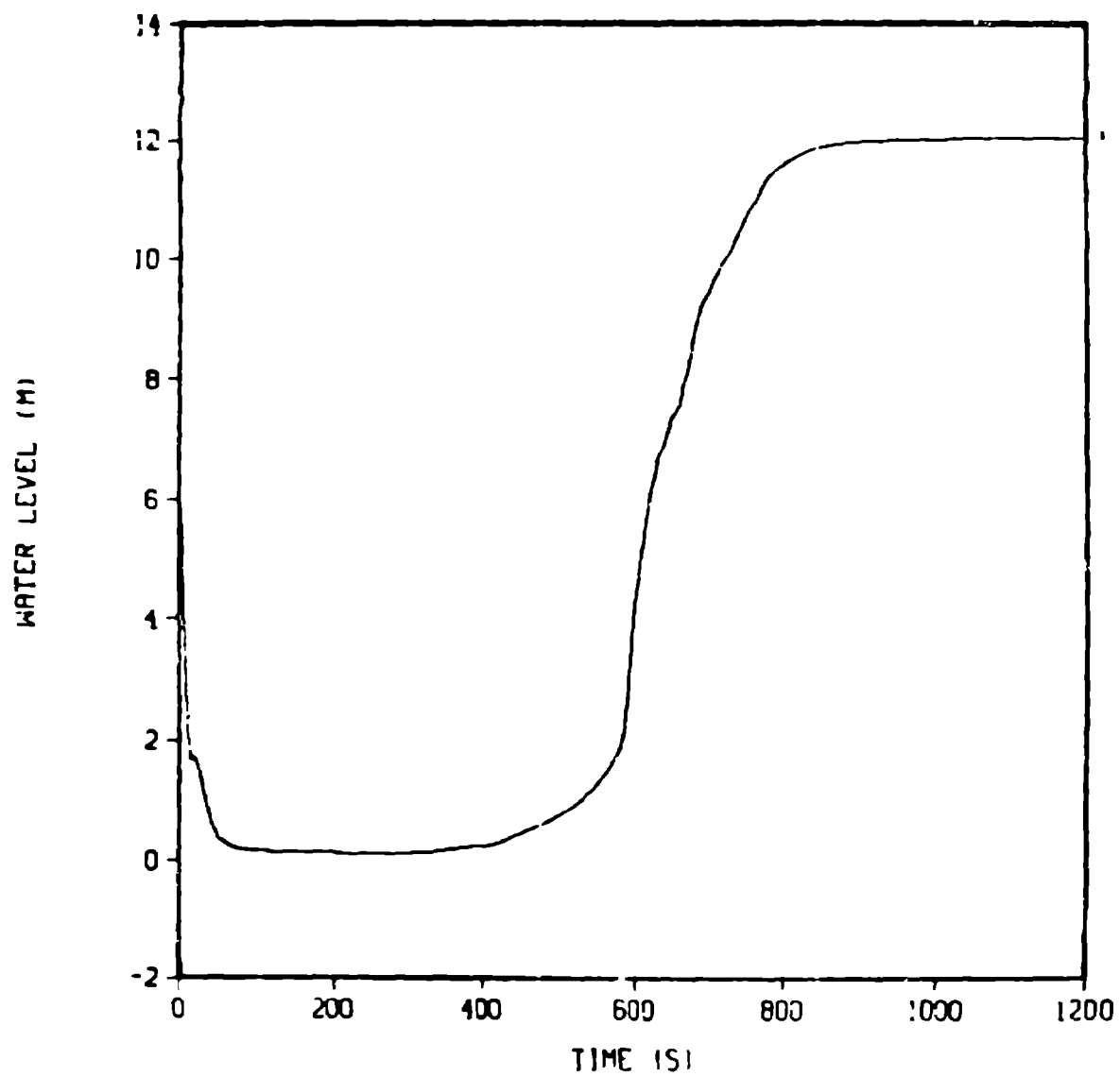
TCE
PRIMARY
ID - 16

Fig. 16



VESSEL
10 - 69

Fig. 10



CELL
1

PRIZER
10 - 22

21

Fig. 22

Fig. 22

R	TH	Z
2	1	3
2	2	3
2	3	3
2	4	3

VESSEL
10 - 69

